

# Three Low-Dimensional Tin Oxalate and Tin Phosphate Materials: BING-4, -7, and -8

Tolulope O. Salami, Kiril Marouchkin, Peter Y. Zavalij, and Scott R. J. Oliver\*

Department of Chemistry, State University of New York at Binghamton,  
Binghamton, New York 13902-6016

Received July 2, 2002. Revised Manuscript Received September 24, 2002

A solvothermal pyridine–HF–tin oxalate system has given rise to two new layered and one new chain crystal structures: BING-4, -7, and -8. BING-4 [SUNY at Binghamton, Structure No. 4,  $\text{Sn}(\text{C}_2\text{O}_4)(\text{C}_5\text{H}_5\text{N})$ , triclinic,  $P-1$ ,  $a = 5.4202(6)$  Å,  $b = 8.3824(9)$  Å,  $c = 9.3506(10)$  Å,  $\alpha = 87.982(2)$ °,  $\beta = 87.916(2)$ °,  $\gamma = 85.650(2)$ °,  $Z = 2$ ] consists of charge-neutral chains of alternating tin and oxalate groups, with pyridine molecules completing the fifth coordination of the tin centers and capping the chains. Both BING-7 ( $[\text{Sn}(\text{C}_2\text{O}_4)\text{F}^-][\text{NH}_4^+]$ , monoclinic,  $P2_1/c$ ,  $a = 8.2736(4)$  Å,  $b = 9.6386(5)$  Å,  $c = 7.7473(4)$  Å,  $\beta = 111.229(1)$ °,  $Z = 4$ ) and BING-8 ( $[\text{Sn}(\text{PO}_4\text{H})\text{F}^-][\text{NH}_4^+]$ , orthorhombic,  $Pnma$ ,  $a = 6.6789(4)$  Å,  $b = 5.3402(4)$  Å,  $c = 15.2795(10)$  Å,  $Z = 4$ ) are anionic, fluorinated, tin oxalate and tin phosphate layers, respectively, with interlamellar charge-balancing ammonium cations. Characterization methods included single-crystal X-ray diffraction (SC-XRD), powder X-ray diffraction (PXRD), in-situ variable temperature (VT) PXRD, thermogravimetric analysis (TGA), and scanning electron microscopy (SEM). The multianalytical data indicate the structures collapse in the 200 °C range, losing their capping or interlamellar species. These Sn(II) materials extend the known chemistry of low-dimensional tin-based structures, and may be useful intercalation compounds.

## Introduction

We are focusing on the solvothermal synthesis and characterization of extended, highly stable oxides and fluorides of germanium, tin, and lead. Our interest in these compositions centers on their potential to generate new open, microporous structures, where we can dictate an anionic or cationic charge on the host. We therefore use both cationic and anionic structure-directing agents (SDAs) in our systems, where the host complements the charge of the SDA. We recently reported a cationic lead fluoride material with anionic SDA, where the latter is nitrate and can be anion-exchanged for dichromate.<sup>1</sup> This unusual anion-based property may give rise to other potential applications, including anion-based catalysis or anion trapping.

We have utilized this largely unexplored methodology with other anionic species that have the potential to act as SDAs. The alkali salts of tetrafluoroborate, in combination with tin oxalate, yielded two new alkali metal–fluoride–tin oxalate framework materials.<sup>2,3</sup> In this instance,  $\text{BF}_4^-$  did not act as SDA, but instead as the source of fluoride. We have also worked extensively with phosphonic acids, which in all cases are not extraframework, as we had desired. Rather, the phosphonate

bonded with the metal centers to generate novel layered Ge-, Sn-,<sup>4</sup> or Pb-based phosphonates.<sup>5</sup> The phenyl rings of the phenylphosphonates cap the  $\text{SnPO}_3$  layers and define an interdigitated bilayer region.

Many tin oxalate and tin phosphate/phosphonate materials have been reported in the literature in recent years.<sup>2–4,6–19</sup> For the former, the bidentate oxalates

(4) Lansky, D. E.; Zavalij, P. Y.; Oliver, S. R. J. *Acta Cryst.* **2001**, *C57*, 1051.

(5) Tran, D. T.; Kam, Y.-S.; Zavalij, P. Y.; Oliver, S. R. J.; submitted for publication.

(6) Ayyappan, S.; Cheetham, A. K.; Natarajan, S.; Rao, C. N. R. *Chem. Mater.* **1998**, *10*, 3746.

(7) Natarajan, S.; Vaidhyanathan, R.; Rao, C. N. R.; Ayyappan, S.; Cheetham, A. K. *Chem. Mater.* **1999**, *11*, 1633.

(8) Audebrand, N.; Vaillant, M.-L.; Auffreric, J.-P.; Louer, D. *Solid State Scie.* **2001**, *3*, 483.

(9) Ayyappan, S.; Cheetham, A. K.; Natarajan, S.; Rao, C. N. R. *Solid State Chem.* **1998**, *139*, 207.

(10) Natarajan, S.; Cheetham, A. K. First Example of a Tin(II) Oxy-Phosphate with an Open-Framework Structure: Synthesis and Structure of  $[\text{NH}_4^+]_2[\text{Sn}_3\text{O}_2(\text{PO}_4)_3]$ . *J. Solid State Chem.* **1997**, *134*, 207.

(11) Natarajan, S.; Cheetham, A. K. *J. Solid State Chem.* **1998**, *140*, 435.

(12) Ayyappan, S.; Bu, X.; Cheetham, A. K. A simple ladder tin phosphate and its layered relative. *Chem. Commun.* **1998**, *20*, 2181.

(13) Natarajan, S.; Ayyappan, S.; Cheetham, A. K.; Rao, C. N. R. Novel Open-Framework Tin(II) Phosphate Materials Containing Sn–O–Sn Linkages and Three-Coordinated Oxygens. *Chem. Mater.* **1998**, *10*, 1627.

(14) Natarajan, S.; Eswaramoorthy, M.; Cheetham, A. K.; Rao, C. N. R. A three-dimensional open-framework tin(II) phosphate exhibiting reversible dehydration and ion-exchange properties. *Chem. Commun.* **1998**, *15*, 1561.

(15) Ayyappan, S.; Chang, J.-S.; Stock, N.; Hatfield, R.; Rao, C. N. R.; Cheetham, A. K. Synthesis, characterization and acid–base catalytic properties of ammonium-containing tin(II) phosphates:  $[\text{NH}_4^+]_2[\text{Sn}_3\text{P}_3\text{O}_12]$  and  $[\text{NH}_4^+]_2[\text{SnPO}_4]$ . *Int. J. Inorg. Mater.* **2000**, *2*, 21.

(16) Liu, Y.-L.; Zhu, G.-S.; Chen, J.-S.; Na, L.-Y.; Hua, J.; Pang, W.-Q.; Xu, R. *Inorg. Chem.* **2000**, *39*, 1820.

\* To whom correspondence should be addressed. Phone: 607-777-4478. Fax: 607-777-2752. E-mail: soliver@binghamton.edu.

(1) Tran, D. T.; Zavalij, P. Y.; Oliver, S. R. J. *J. Am. Chem. Soc.* **2002**, *124*, 3966.

(2) Salami, T. O.; Zavalij, P. Y.; Oliver, S. R. J. *Acta Cryst.* **2001**, *E57*, m111.

(3) Salami, T. O.; Zavalij, P. Y.; Oliver, S. R. J. *Acta Cryst.* **2001**, *E57*, i49.

**Table 1. Summary of Synthesis Conditions and Major Products**

no.	molar ratios (Py = pyridine, C <sub>5</sub> H <sub>5</sub> N)	synthesis time (days)	synthesis temp. (°C)	major phase(s) observed in PXRD
1	20 Py:4 H <sub>2</sub> O:1 HF:1 CF <sub>3</sub> SO <sub>3</sub> H:1 Sn(C <sub>2</sub> O <sub>4</sub> ) <sup>a</sup>	5	125	BING-4
2	20 Py:4 H <sub>2</sub> O:1 HF:1 CF <sub>3</sub> SO <sub>3</sub> H:1 Sn(C <sub>2</sub> O <sub>4</sub> )	5	100	some BING-4
3	20 Py:4 H <sub>2</sub> O:1 HF:1 CF <sub>3</sub> SO <sub>3</sub> H:1 Sn(C <sub>2</sub> O <sub>4</sub> )	5	150	some BING-4
4	20 Py:4 H <sub>2</sub> O:1 HF:1 CF <sub>3</sub> SO <sub>3</sub> H:1 Sn(C <sub>2</sub> O <sub>4</sub> )	5	175	unknown phase
5	20 Py:4 H <sub>2</sub> O:1 HF:1 CF <sub>3</sub> SO <sub>3</sub> H:1 Sn(C <sub>2</sub> O <sub>4</sub> )	3	125	unknown phase
6	20 Py:4 H <sub>2</sub> O:1 HF:1 CF <sub>3</sub> SO <sub>3</sub> H:1 Sn(C <sub>2</sub> O <sub>4</sub> )	4	125	some BING-4
7	20 Py:4 H <sub>2</sub> O:1 HF:1 Sn(C <sub>2</sub> O <sub>4</sub> )	5	125	unknown phase
8	20 Py:1 H <sub>2</sub> O:1 HF:1 NH <sub>4</sub> C <sub>2</sub> O <sub>4</sub> ·H <sub>2</sub> O (Acros)	4 to 5	150	BING-7
9	20 Py:1 H <sub>2</sub> O:1 HF:1 NH <sub>4</sub> C <sub>2</sub> O <sub>4</sub> ·H <sub>2</sub> O (Acros)	5	125	some BING-7
10	20 Py:1 H <sub>2</sub> O:1 HF:1 NH <sub>4</sub> C <sub>2</sub> O <sub>4</sub> ·H <sub>2</sub> O (Acros)	5	100	unknown phase
11	20 Py:1 H <sub>2</sub> O:1 HF:1 NH <sub>4</sub> C <sub>2</sub> O <sub>4</sub> ·H <sub>2</sub> O (Acros)	5	175	unknown phase
12	20 Py:10 H <sub>2</sub> O:2 HF:1 PF <sub>6</sub> NH <sub>4</sub> :1 SnF <sub>2</sub> <sup>c</sup>	5	150	BING-8
13	20 Py:10 H <sub>2</sub> O:2 HF:1 PF <sub>6</sub> NH <sub>4</sub> :1 SnF <sub>2</sub>	3 to 4	150	some BING-8
14	20 Py:10 H <sub>2</sub> O:2 HF:1 PF <sub>6</sub> NH <sub>4</sub> :1 SnF <sub>2</sub>	5	125	some BING-8
15	20 Py:10 H <sub>2</sub> O:2 HF:1 PF <sub>6</sub> NH <sub>4</sub> :1 SnF <sub>2</sub>	5	100	unknown phase
16	20 Py:10 H <sub>2</sub> O:2 HF:1 PF <sub>6</sub> NH <sub>4</sub> :1 SnF <sub>2</sub>	5	175	unknown phase
17	20 Py:5 H <sub>2</sub> O:2 HF:1 PF <sub>6</sub> NH <sub>4</sub> :1 SnF <sub>2</sub>	5	150	some BING-8
18	10 Py:10 H <sub>2</sub> O:2 HF:1 PF <sub>6</sub> NH <sub>4</sub> :1 SnF <sub>2</sub>	5	150	trace of BING-8
19	20 Py:1 H <sub>2</sub> O:2 HF:1 PF <sub>6</sub> NH <sub>4</sub> :1 SnF <sub>2</sub>	5	150	some BING-8

<sup>a</sup> CF<sub>3</sub>SO<sub>3</sub>H (Acros, 99%). <sup>b</sup> NH<sub>4</sub>C<sub>2</sub>O<sub>4</sub>·H<sub>2</sub>O (Acros). <sup>c</sup> PF<sub>6</sub>NH<sub>4</sub> (Acros, 99.5%).

always three-connect the octahedral tin centers into layers.<sup>4,6–8</sup> Tin phosphate/phosphonate materials, on the other hand, can be clusters<sup>9</sup> or extended in two<sup>10–12</sup> or three dimensions.<sup>13–19</sup> The majority of these structures were reported by Cheetham and co-workers.<sup>6,7,9–15,17–19</sup> In all cases, cationic interlayer or extraframework groups – in most cases protonated amines – reside in the void space of these structures. Note the absence of one-dimensional chain structures from this class of compounds.

Here, we report the solvothermal synthesis and physical characterization of three new tin-based low-dimensional crystal structures. All were isolated from related pyridine solvent systems. The layered materials show typical oxalate or phosphate connectivity, and expected thermal behavior. The tin oxalate chain structure, to our knowledge, is the first of its kind.

## Experimental Section

**Synthetic Procedure.** A typical experiment included the following reagents (all used as-received): (i) pyridine solvent (Acros, 99%); (ii) hydrofluoric acid (49% aqueous, Fisher); (iii) tin(II) oxalate or fluoride (Gelest); (iv) the structure directing agent (see Table 1). These chemicals were added sequentially to a 250-mL Nalgene beaker, with thorough manual mixing after each step. After mechanical stirring for an additional 10 min, the opaque, viscous mixture was sealed in a 23-mL-capacity Teflon-lined autoclave (constructed in-house) and heated statically. The resultant products were suction-filtered and washed with acetone (all products) and water (BING-8). The ideal synthetic conditions were as follows (Table 1): BING-4, expt. #1, yield 79.3%; BING-7, expt. #8, yield 83.4%; BING-8, expt. #12, yield 53.8%.

**Characterization Methods.** Powder X-ray diffraction (PXRD) was performed on a Scintag XDS 2000 diffractometer with Cu K $\alpha$  radiation ( $\lambda = 1.5418 \text{ \AA}$ ), solid-state detector (which removes white radiation and  $\beta$  lines), scan range of 2°

to 45° (20), step size 0.02°, and scan rate 4.0°/min. All samples were ground thoroughly in a mortar and pestle before mounting the resultant powder in the PXRD sample holder. TGA was performed on a TA Instruments 2950, with a 10 °C/min scan rate and nitrogen purge. SC-XRD was on a Bruker AXS single-crystal diffractometer with Smart Apex detector, Mo K $\alpha$  graphite monochromated radiation ( $\lambda = 0.71073 \text{ \AA}$ ),  $\omega$ -scan,  $\omega$  step size 0.3° and 10 s exposure time, absorption correction using SADABS.<sup>20</sup> SEM was done on an ETEC Autoscanner SEM. All specimens were coated with gold (Au) using a Denton Vacuum Inc. Desk 1 sputter coater. Operating conditions were 5 kV, 13-mm working distance (BING-4 and -7); 10 kV, 18-mm working distance (BING-8).

## Results and Discussion

**Tin Oxalate Chain, BING-4.** This structure, to our knowledge, is the first example of a one-dimensionally extended tin oxalate. The experimental and crystallographic parameters are summarized in Tables 1 and 2, respectively. The material can be synthesized within the temperature range of 100 to 150 °C (expts 1–3, Table 1), but higher temperatures yielded an unknown phase with only higher angle peaks (expt 4).<sup>21</sup> The chain structure consists of alternating tin and oxalate groups [Sn(C<sub>2</sub>O<sub>4</sub>)(C<sub>5</sub>H<sub>5</sub>N), Figure 1]. The tin centers connect to four oxygens of their two neighboring oxalate groups (Figure 1a,b). The Sn–O bond lengths range from 2.151(2) Å to 2.533(2) Å (Table 3). The pyridine solvent for this experiment acted as ligand, connecting to Sn through its nitrogen [Sn–N 2.484(2) Å]. The pyridine rings therefore cap the chains, and also interdigitate with those of the neighboring chains (Figure 1a). The chains zigzag along the *b*-axis, and the geometry of the five-coordinate Sn's are distorted, umbrella-like (Figure 1b). The other side of the Sn is likely a lone pair of electrons, but could not be resolved by SC-XRD. The stereochemically active lone pair of electrons leads to unpredictable coordination geometries for Sn and Pb.<sup>1–19</sup> Interestingly, triflic acid was necessary in order to

(17) Ayyappan, S.; Bu, X.; Cheetham, A. K.; Rao, C. N. R. Synthesis and Structural Characterization of a Chiral Open-Framework Tin(II) Phosphate, [CN<sub>3</sub>H<sub>6</sub>][Sn<sub>4</sub>P<sub>3</sub>O<sub>12</sub>] (GUAN–SnPO). *Chem. Mater.* **1998**, *10*, 3308.

(18) Adair, B.; Natarajan, S.; Cheetham, A. K. Synthesis and structural characterization of a novel tin(II) phosphonate, Sn<sub>2</sub>(O<sub>3</sub>PCH<sub>3</sub>)(C<sub>2</sub>O<sub>4</sub>). *J. Mater. Chem.* **1998**, *8*, 1477.

(19) Stocka, N.; Stucky, G. D.; Cheetham, A. K. The hybrid open-framework of tin(II) phosphonopropionate oxalate, Sn<sub>4</sub>(O<sub>3</sub>PCH<sub>2</sub>CH<sub>2</sub>CO<sub>2</sub>)<sub>2</sub>(C<sub>2</sub>O<sub>4</sub>). *Chem. Commun.* **2000**, 2277.

(20) Sheldrick, G. M. SADABS. University of Göttingen, Germany, 1996.

(21) Because of the absence of lower angle peaks, we presume this solid is a condensed oxide phase. Also note that no solid was formed in the absence of triflic acid (expt 7), even though it does not end up in the final structure.

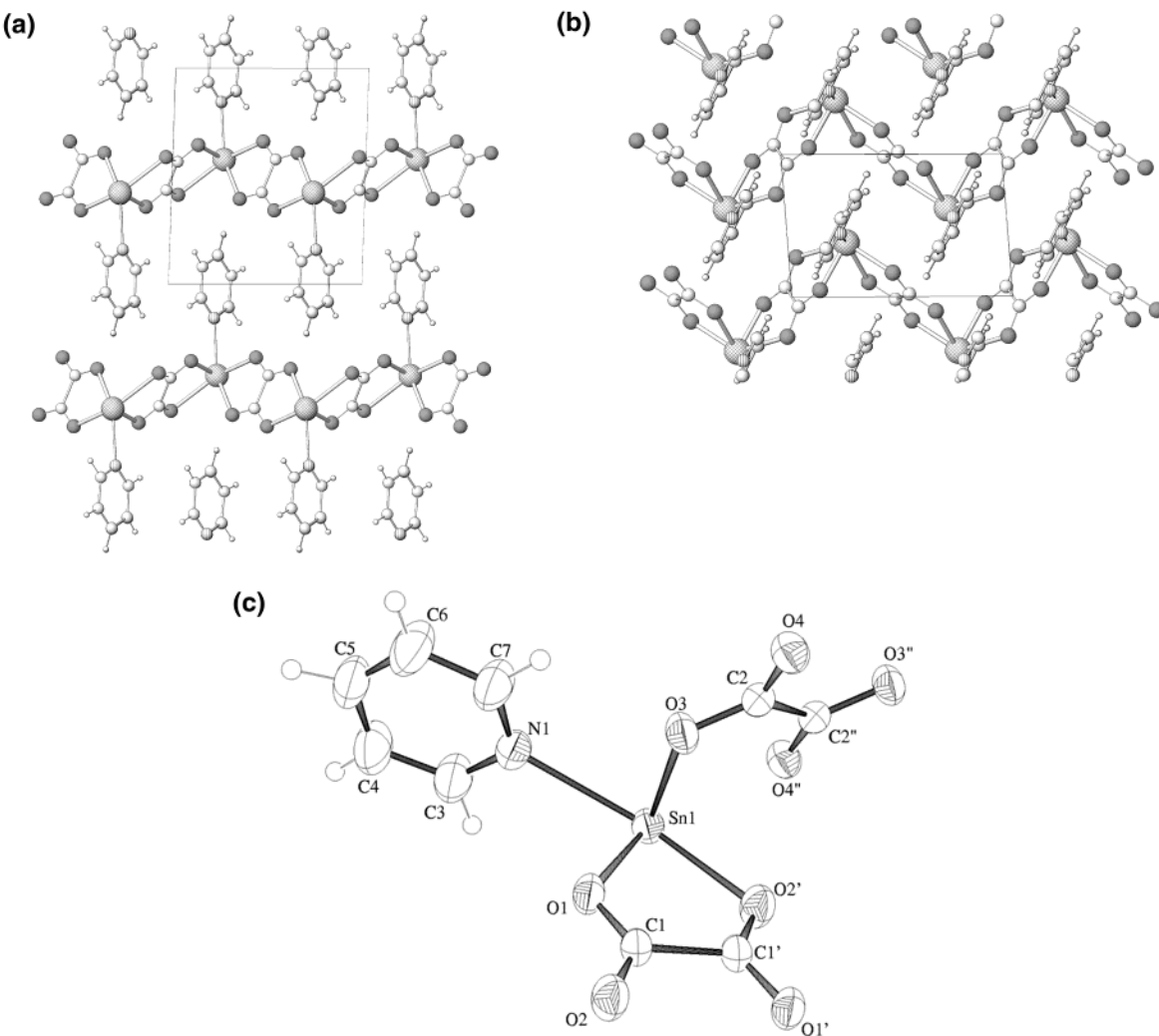


**Figure 1.** Crystal structure of BING-4 [ $\text{Sn}(\text{C}_2\text{O}_4)(\text{C}_5\text{H}_5\text{N})$  - Sn, hatched circles; O, light gray circles; C, large open circles; H, small open circles; N, vertical stripes]: (a) the  $a$ -projection shows the interdigititation of the tin oxalate chains; (b) the corrugated chains extend along the  $b$ -axis; and (c) thermal ellipsoids and labeling scheme, shown at 50% probability levels.

obtain BING-4 (Table 1). It is possible that triflate ligates the tin centers during the reaction,<sup>22</sup> allowing a low-dimensional solvent-capped chain to be formed.

**Tin Oxalate Layer, BING-7.** Ammonium is a very commonly occurring extraframework cation for extended tin phosphates,<sup>10,15</sup> as well as the oxides of earlier Group 14 metals.<sup>23,24</sup> BING-7,  $[\text{Sn}(\text{C}_2\text{O}_4)\text{F}^-][\text{NH}_4^+]$ , is an anionic layer with interlayer ammonium cations, and one terminal fluoride on each tin center (Figure 2). The Sns are distorted six-coordinate, bonding to five oxygens of three different oxalate groups (Table 3). The oxalate oxygens in this case are three-coordinate, bonding to the oxalate carbon and two Sn centers (Figure 2a). One oxygen of each oxalate is terminal, and the ammonium groups occupy the interlamellar space (Figure 2b). BING-7 was synthesized at 150 and 125 °C (expts 8 and 9, Table 1), again with an unknown condensed product

**Table 2. Summary of Crystal Data, Details of Intensity Collection, and Refinement**

	BING-4	BING-7	BING-8
empirical formula	$\text{H}_5\text{C}_7\text{NO}_4\text{Sn}$	$\text{H}_4\text{C}_2\text{NO}_4\text{FSn}$	$\text{H}_5\text{FNO}_4\text{PSn}$
formula weight	285.81	243.75	251.71
crystal size (mm)	$0.10 \times 0.24 \times 0.24$	$0.40 \times 0.31 \times 0.22$	$0.48 \times 0.19 \times 0.09$
crystal system	triclinic	monoclinic	orthorhombic
space group	P-1	$P2_1/c$	Pnma
color of crystal	colorless	colorless	colorless
$a$ (Å)	5.4202(6)	8.2736(4)	6.6789(4)
$b$ (Å)	8.3824(9)	9.6386(5)	5.3402(4)
$c$ (Å)	9.3506(10)	7.7473(4)	15.2795(10)
$\alpha$ (deg)	87.982(2)	90	90
$\beta$ (deg)	87.916(2)	111.229(1)	90
$\gamma$ (deg)	85.650(2)	90	90
$V$ (Å <sup>3</sup> )	423.11(8)	575.89(5)	544.97(6)
$Z$	2	4	4
$T$ (K)	293(2)	110(2)	293(2)
$D_C$ (g cm <sup>-3</sup> )	2.243	2.811	3.068
$\mu(\text{Mo K}\alpha)$ (mm <sup>-1</sup> )	2.998	4.401	4.935
min. $\mu$ correction (mm <sup>-1</sup> )	0.581	0.275	0.339
max. $\mu$ correction (mm <sup>-1</sup> )	0.741	0.380	0.648
no. of obsd data	2241	1817	854
$[I > 2\sigma(I)]$			
$R_1$ $[I > 2\sigma(I)]$	0.0281	0.0273	0.0264
$wR_2$ (all data)	0.0630	0.0637	0.0646
goodness of fit	0.972	1.075	1.034

(22) Triflate is well-known in organometallic chemistry to complex a variety of metals, including Sn. Hitchcock, P. B.; Lappert, M. F.; Lawless, G. A.; de Lima, G. M.; L. Pierssens, J.-M. *J. Organomet. Chem.* **2000**, *601*, 142.

(23) Szostak, R. *Molecular Sieves: Principles of Synthesis and Identification*, 2nd ed.; Chapman & Hall: New York, 1998.

(24) See, for example: Cascales, C.; Gutierrez-Puebla, E.; Monge, M. A.; Ruiz-Valero, C.  $(\text{NH}_4)_2\text{Ge}_2\text{O}_{15}$ : A Microporous Material Containing  $\text{GeO}_4$  and  $\text{GeO}_6$  Polyhedra in Nine-Rings. *Angew. Chem., Int. Ed.* **1998**, *37*, 129.

**Table 3. Selected Bond Lengths (Å) and Bond/Torsion Angles (deg) for Each Structure**

BING-4	BING-7	BING-8			
Sn1–O3	2.151(2)	Sn1–F1	2.0437(19)	Sn1–F1	2.036(3)
Sn1–O1	2.2687(19)	Sn1–O1	2.230(2)	Sn1–O2	2.1241(19)
Sn1–O2	2.377(2)	Sn1–O3	2.241(2)	P1–O1	1.516(3)
Sn1–O4	2.533(2)	C1–O2	1.229(3)	P1–O2	1.5356(19)
Sn1–N1	2.484(2)	C1–O1	1.283(3)	P1–O3	1.572(3)
C1–C1	1.554(5)	C1–C2	1.560(4)		
O1–C1	1.255(3)	C2–O4	1.223(3)		
O2–C1	1.239(3)	C2–O3	1.291(3)	F1–Sn1–O2	84.95(8)
O3–C2	1.269(3)			O2–Sn1–O2	84.39(10)
O4–C2	1.231(3)	F1–Sn1–O1	84.79(8)	O1–P1–O2	113.25(9)
C2–C2	1.546(5)	F1–Sn1–O3	88.99(8)	O1–P1–O3	109.39(16)
O3–Sn1–O1	80.04(8)	O1–Sn1–O3	71.96(7)	O2–P1–O3	106.16(10)
O3–Sn1–O2	80.93(8)	C1–O1–Sn1	119.54(17)		
O1–Sn1–O2	70.75(6)				
O3–Sn1–N1	77.29(8)	O1–C1–C2–O3	6.6(4)		
O1–Sn1–N1	76.23(7)	O2–C1–C2–O4	6.8(4)		
O2–Sn1–N1	142.98(8)	O1–C1–C2–O4	−173.1(3)		
		O2–C1–C2–O3	−173.4(3)		

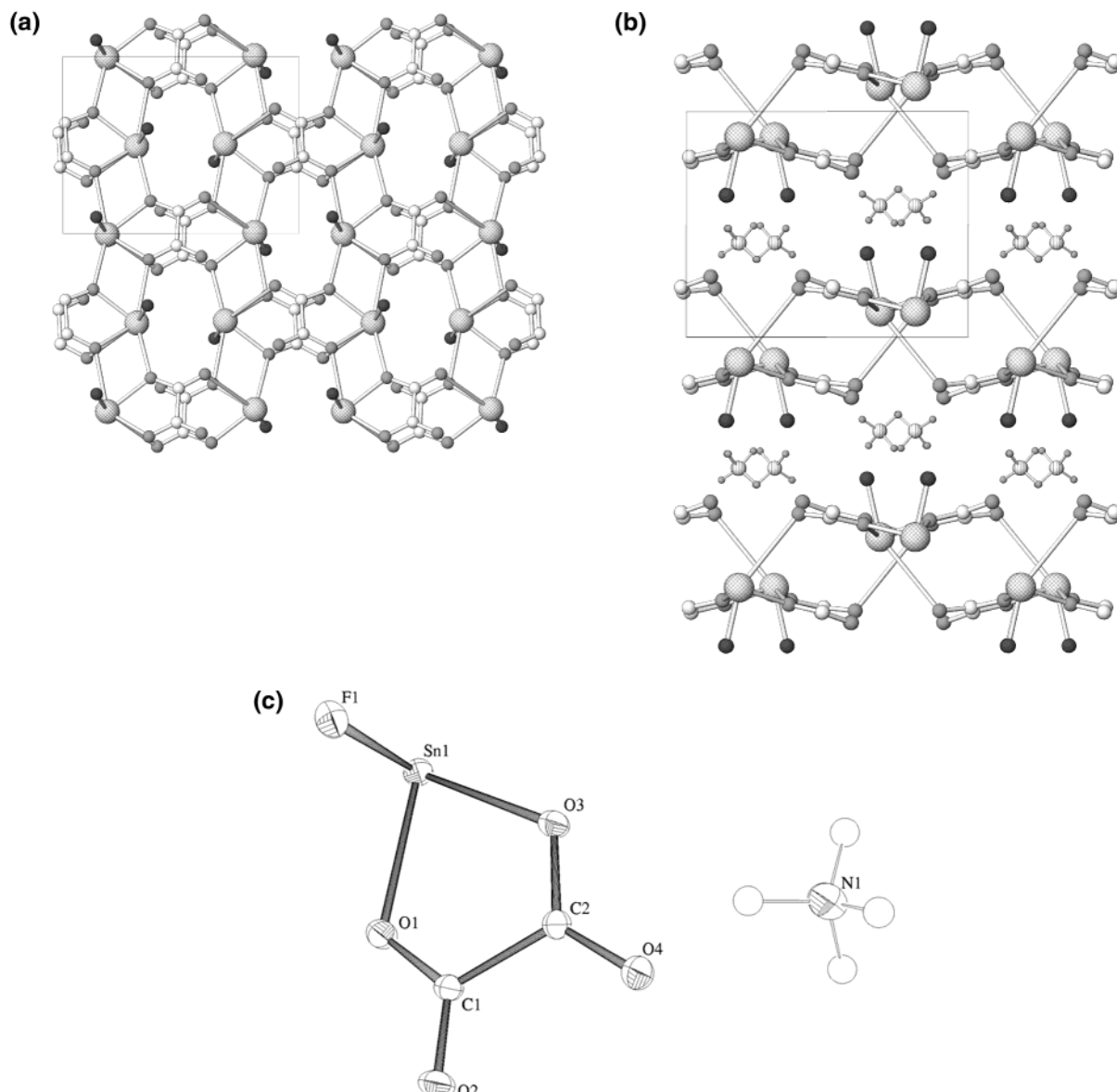


**Figure 2.** Crystal structure of BING-7  $[\text{Sn}(\text{C}_2\text{O}_4)\text{F}^-][\text{NH}_4^+]$  - F, dark gray circles]: (a) the  $\alpha$ -projection of one layer shows the five-coordinate tin centers; (b) the anionic layers are charge-balanced by interlamellar hydroniums; and (c) thermal ellipsoids and labeling scheme, shown at 50% probability levels.

at 100 °C (expt 10) and higher temperatures (expt 11). A structure very closely related to BING-7, at least compositionally, is  $\text{Sn}_2(\text{NH}_4)_2(\text{C}_2\text{O}_4)_3 \cdot 3\text{H}_2\text{O}$ , a layered tin

oxalate.<sup>8</sup> Interestingly, this material was also synthesized with the oxalate salt as the ammonium source. BING-7, however, is fluorinated, and the fluorides cap

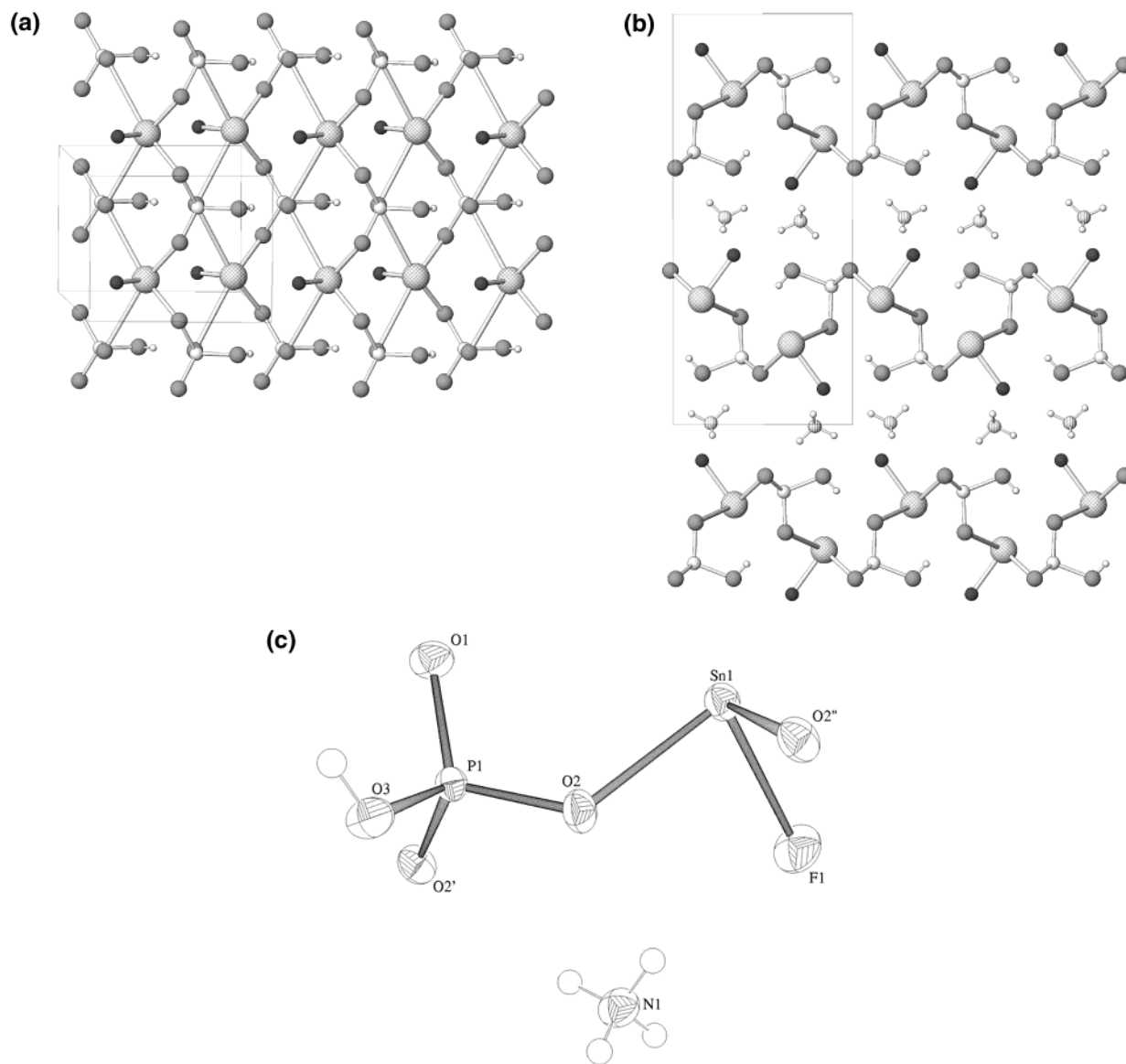


**Figure 3.** Crystal structure of BING-8  $[[\text{Sn}(\text{PO}_4\text{H})\text{F}^-][\text{NH}_4^+]] \cdot \text{P}$ , large open circles]: (a) the tin phosphate layer with terminal fluoride and hydroxide groups; (b) the *b*-projection showing the alternating Sn–O–P–O–Sn sequence in the corrugated layers; and (c) thermal ellipsoids and labeling scheme, shown at 50% probability levels.

the layers and point into the interlamellar region (Figure 2b). The ammoniums are hydrogen-bonded to the terminal fluorides and oxygens of the oxalate groups (Table 4).

**Tin Phosphate Layer, BING-8.** BING-8 is a tin fluorophosphate ( $[\text{Sn}(\text{PO}_4\text{H})\text{F}^-][\text{NH}_4^+]$ ), and is related to BING-7 in that the fluorides reside on Sn, are terminal, and point into the interlayer space (Figure 3). The Sn centers bond to four separate monohydrogen phosphate groups through doubly bridging oxygens (Figure 3a). Two of these bonds are strong [Sn–O 2.124(2) Å], while the other interaction is very weak [Sn–O 3.105(2) Å, Table 3]. Each phosphate group connects to three Sn<sub>4</sub>s, and has one terminal hydroxy group that forms an intralayer hydrogen bond (Figure 3b, Table 4). The interlayer ammonium ions balance the negative charge of, and are involved in strong hydrogen bonding with, the anionic tin fluorophosphate layers (Table 4). Ammonium again acted as charge-balancing cation for this experiment, but was added as its hexafluorophosphate salt (expts 12–19, Table 1).<sup>25</sup> Again, only a

**Table 4. Hydrogen Bond Lengths and Angles for BING-7 and -8**

BING-7			
D–H (Å)	H…A (Å)	D…A (Å)	D–H…A (deg)
N1–H1…F1	0.88(3)	1.95(4)	2.782(3)
N1–H2…O2	0.88(3)	2.13(4)	2.883(4)
N1–H2…F1	0.88(3)	2.61(4)	3.177(3)
N1–H3…O2	0.89(3)	2.01(3)	2.859(4)
N1–H3…O4	0.89(3)	2.42(5)	2.901(4)
N1–H4…F1	0.89(3)	1.98(3)	2.865(4)
BING-8			
D–H (Å)	H…A (Å)	D…A (Å)	D–H…A (deg)
O3–H3…O1	0.74(5)	1.85(5)	2.581(4)
N1–H2A…F1	0.790(10)	2.001(11)	2.790(4)
N1–H1A…F1	0.788(8)	2.270(9)	3.031(2)
N1–H1A…O2	0.788(8)	2.558(15)	3.092(4)

narrow solvothermal temperature range leads to this structure, presumably due to the metastability of the structures and their tendency to form condensed phase tin oxide.

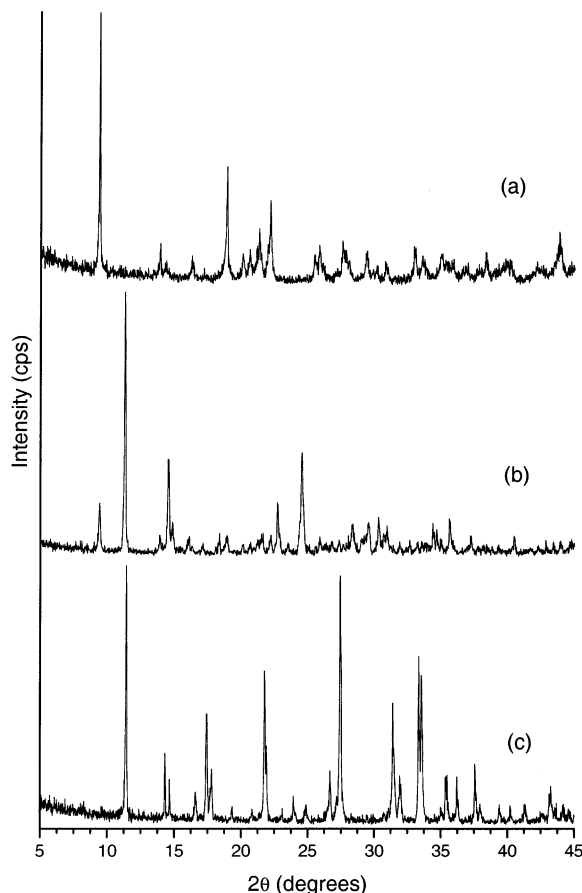


**Figure 4.** PXRD patterns for products formed under the ideal conditions (Table 1): (a) BING-4; (b) BING-7; and (c) BING-8.

**Physical Characterization.** BING-4, -7, and -8 were each studied by PXRD (Figure 4), SEM (Figure 5), TGA, and VT-PXRD. PXRD confirmed that all three as-synthesized materials are phase-pure, compared to the theoretical pattern projected from single-crystal data. SEM data shows the larger crystal size and well-defined morphology of the tin phosphate crystals (BING-8, Figure 5c), versus those of the tin oxalates (Figure 5a,b).

The weight-loss temperatures observed in the TGA experiments correlated with changes in the powder patterns observed in the VT-PXRD runs. Each material shows minor weight loss events up to 100 °C (less than 3 wt %). BING-4 transformed to low-crystallinity<sup>26</sup> tin oxide (cassiterite form of  $\text{SnO}_2$ , JC-PDS ref. 03-0439) at approximately 325 °C, losing the carbon of the oxalates and the pendant pyridine groups (experimental weight loss, 36.5 wt %; theoretical, 36.0 wt %). BING-7 also lost its oxalate carbons and interlamellar ammoniums, decomposing to a similar tin oxide material around 210 °C (experimental 37.0 wt %; theoretical 38.2 wt %). We believe that the material was oxidized by impure house nitrogen and/or due to the diffusion of outside air into the TGA chamber.

(25) We were attempting to use  $\text{PF}_6^-$  as an anionic SDA, but instead  $\text{NH}_4^+$  acted as extraframework cation.  $\text{PF}_6^-$  did not appear in the resultant solid.

(26) The low crystallinity manifested itself in the low intensity and breadth of the PXRD peak.

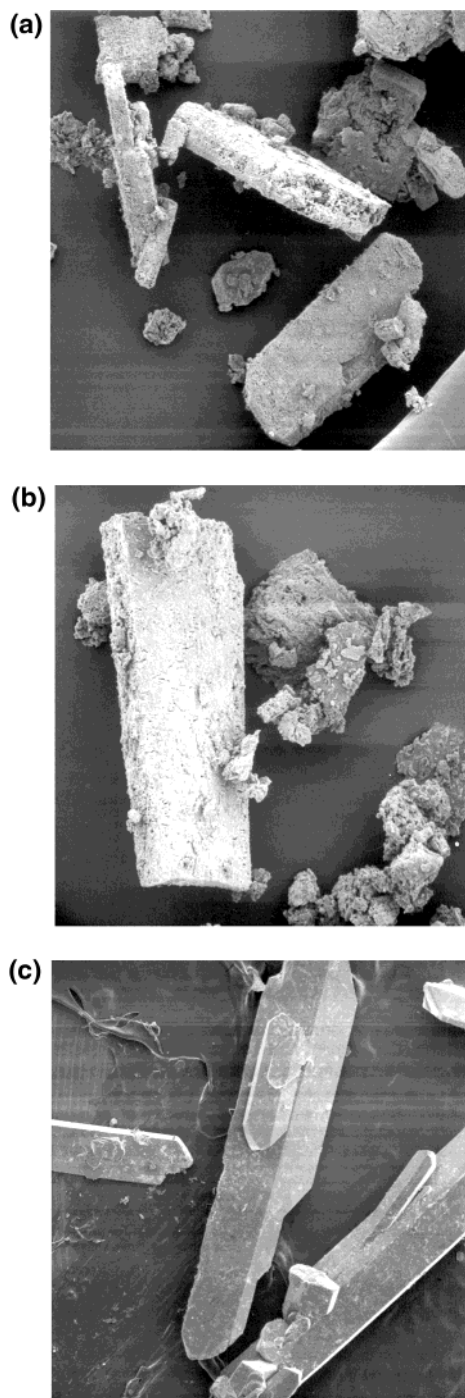


**Figure 5.** SEM of the tin-based crystals: (a) BING-4 (magnification 500×); (b) BING-7 (magnification 1000×); and (c) BING-8 (magnification 30×).

BING-8, the tin phosphate, does not contain oxalate groups and therefore did not show as significant a decrease in weight percent. The PXRD pattern became amorphous, decomposing around 200 °C. Presumably, the material lost its ammoniums, judging by the TGA-observed weight loss (experimental 22.3 wt %). Preliminary tests on cation-exchange were unsuccessful. We attempted to exchange the ammonium groups for TMA, expecting an increase in interlayer distance. After several days of stirring the material in 1.0 M TMA-OH solution, however, the PXRD pattern remained unchanged. We are currently studying our new tin oxalates and phosphates for their intercalation properties.

### Conclusions

The crystal structures reported here further demonstrate the structural diversity possible in these systems, and more structure-types are anticipated. This paper represents the first example of a polymeric tin oxalate material, as well as the first report of pyridine as a reaction medium for these compositions. All of these structures contain Sn(II) centers. We are currently extending our studies to the tin(IV) system. Circumventing the inert pair effect of tin to give the +4 oxidation state has been shown for the amine-templated tin sulfide materials of Ozin and co-workers.<sup>27</sup> By

working with this higher oxidation state, we believe we can isolate open-framework tin oxides for molecular sieving and possibly semiconducting applications.

**Acknowledgment.** We thank the donors of the Petroleum Research Fund, Grant 36101-G5, in partial support of this research.

CM020711R

---

(27) Bowes, C. L.; Petrov, S.; Vovk, G.; Young, D.; Ozin, G. A.; Bedard, R. L. *J. Mater. Chem.* **1998**, *8*, 711–720, and references therein.